Modelling and Analysis of Geodesic Structures

Raquel Vestia Ribeiro[a,*]

[a]*Instituto Superior Técnico, Lisboa, Portugal*

Abstract

The desire to study geodesic structures came from the energetic-synergetic concept, by Buckminster Fuller, defined by triangular geodesic grids of frames and joints. The frequency, V_n, corresponds to the number of divisions, n, made to the initial triangle. Using Matlab software to design V_n (n=2,4,6,8) geometries two different scenarios were evaluated: one where the structures are at surface level exposed to wind (case study 1) and another where the structures are underground and subjected to the ground pressure above it (case study 2). The Finite Element Method (from Sap2000 and Inventor) is the method used to design and perform the analysis of both scenarios allowing to simulate mechanical characteristics, behaviours and complex geometries. The structural elements are designed: shells, frames and joints, complying with ULS and SLS limit states according to the corresponding Eurocodes. The materials used in the design of the models are steel, bamboo and wood. The bottom line in both scenarios is that all the models are more affected by the bending effect than by the tensile/compression forces, regarding the shell and frame elements. It's also possible to use wood as a structural material if the forces and the environmental conditions are within a reasonable level. Otherwise, for other situations with a higher level of forces, steel remains a valid option, since it's a strong and resistant material. The joints are mainly subjected to axial forces due to the frames, where bamboo has proven to be a material with a adequate behaviour to withstand those forces.

Keywords: Structural design, Geodesic Structures, Geodesic domes

1. Introduction

In the late XX century, Buckminster Fuller popularized into construction the possibility of creating spherical or hemispherical structures, based on a grid of triangles, defined by articulated frames and joints. This affinity arose from the need to create a natural and organic form, which gave birth to the "energetic-synergetic" concept. On one hand, Energetic, derives from the fact that Nature tends to build the lightest, self-balanced and efficient structures, taking as an example the case of molecules. On the other, Synergetic, stands from the point where the global behaviour of each system cannot be analysed solely based on the behaviour of each individual element in its constitution [1]. Figure 1 to 3 show three of the greatest examples of geodesic structures around the world.

The design of domes is built from three types of platonic solids: the tetrahedron, the octahedron and the icosahedron, the latter being the base for this master dissertation. The process consists of dividing each area of the icosahedron in equal and equilateral triangles, while projecting its vertices coinciding to the outer sphere.

The greatest the area subdivision, the more triangles are obtained and, therefore, more areas exist within the geodesic grid, which implies a much more spherical form. The geodesic frequency, V_n, takes its name from the characteristic value, n, that determines the number of structural subdivisions for each triangle of the geodesic grid. In this way, geodesic geometries were developed with high structural stiffness and strength, which results from the combination of its individual elements. To better understand the behaviour of geodesic and hemispherical structures in different scenarios, namely, at the surface level and underground, it is necessary to design them in order to withstand the wind and soil pressure loads, respectively. Comparisons are made for each of these scenarios, in structures with the same base area reference, while varying the frequency from V2 to V8 (only even numbers). These designs are made with materials such as steel, bamboo and timber, while following the guidelines and regulations of the according Eurocodes. For the rupture of bamboo, a general von Mises stress criteria is considered. The geometry of each model is taken from a code generated in Matlab. The formulation of each model is made accordingly to the Finite Element Method (FEM) which is the best solution to evaluate the structural behaviour of each scenario in programs such as SAP2000 and Inventor, since they allow to simulate much more complex mechanic properties and geometries.

*

Email address: raquelvestia@tecnico.ulisboa.pt (Raquel Vestia Ribeiro)

Figure 1: Poliedro de Caracas ©Flickr Werner Ustorf

Figure 2: Montreal Biosphére ©Flickr Herbert Plagge

Figure 3: The Eden Project ©Flickr Metropanas

2. Geometry Design

To generate the geodesic domes, an algorithm [2] is used, which allows to extract automatically both the coordinates of each geodesic vertices, and also the corresponding triangulations according to the Delaunay method. This method demonstrates that there is a single triangulation which maximizes the sum of the smallest angles of each triangle. Therefore, the Delaunay triangulation is the one that originates a set of elements that will be the closest possible to equilateral triangles.

The algorithm generated is based on the polyhedron of type icosahedron (class I) with type 1 subdivision, as shown in the Figure 4. The type 1 subdivision corresponds to the division of the original elements with lines parallel to these same elements. In this master dissertation are analysed four different dome models with a fixed radius of 3.75 m and different geodesic frequencies, n, according to Figure 5. The number of elements in each model are shown in Table 1, so that the reader has a better understanding of the influence of a higher frequency in the increasing number of elements.

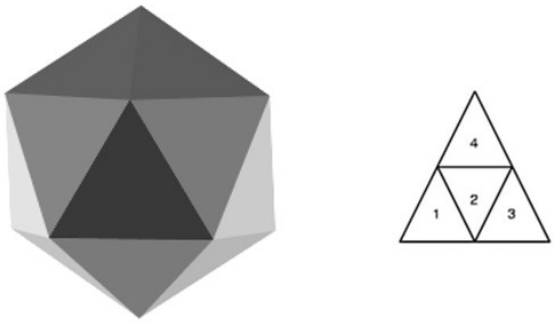

Figure 4: Class I (icosahedron) with type 1 subdivision

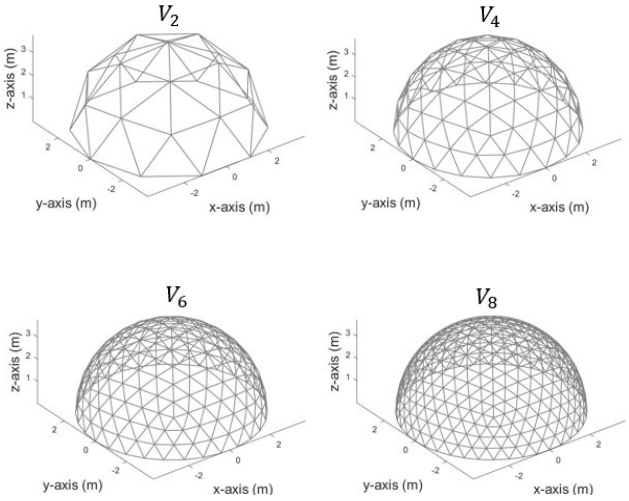

Figure 5: 3D view of each V_n model

Table 1: Number of elements in each dome according to the V_n frequency

	Joints		Frames	Areas
	Total	Base		
V_2	26	10	65	40
V_4	91	20	250	160
V_6	196	30	555	360
V_8	341	60	980	640

3. Case study 1

This case study concerns the geodesic domes placed at the surface level.

Where the combinations of actions for ULS (1) and SLS (2) are:

$$Comb_1 = 1,35 \cdot dead + 1,50 \cdot wind \quad (1)$$

$$Comb_{1,ut} = dead + wind \quad (2)$$

The design was performed for both frame and joint elements. The wind loadings on the structures were quantified accordingly to the corresponding Eurocode, EC1-4 [3].

For estimation of the wind actions, the following parameters were considered:

- Location: Ericeira
- Terrain type B: $v_{b,0} = 30\ m/s$
- $z_e = 3.75\ m$
- $q_p(z_e) = 1.30\ kN/m^2$

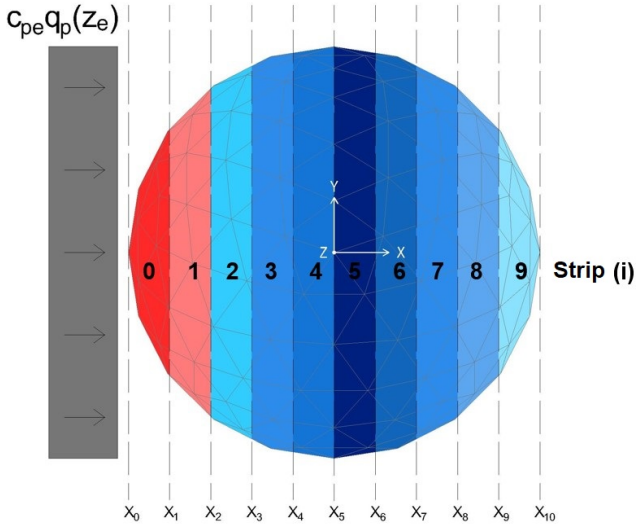

Figure 6: Plan view of the V_4 model with a representation of the exterior pressure coefficients location for each strip

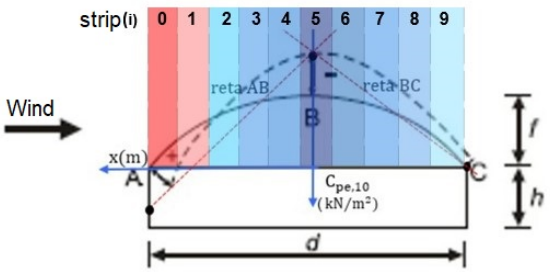

Figure 7: Schematic of the $C_{pe,10}$ table values

Frames

The frame elements are in timber of type C24 with a squared cross section and its design was made according to the general Eurocode EC1 [4] rules, and also the one associated to the type of material, in this case, EC5 [5].

Table 2: Characteristic values for the type C24 timber

$f_{m,k}[N/mm^2]$	24
$f_{t,0,k}[N/mm^2]$	14.5
$f_{c,o,k}[N/mm^2]$	21
$E_{mean}[N/mm^2]$	11 x 10^3
$E_{0,05}[N/mm^2]$	7.4 x 10^3
$\rho[kg/m^3]$	420

- Actions duration class = mín[permanent (dead weight); short term (wind)] = short term
- Service class = 3
- $k_{mod} = 0.70$
- $\gamma_M = 1.30$

The critical section of each frame is the middle section and while evaluating the entire structure, it is verified that the combined state of bending with tension is the most important criteria.

A pre-design was made, starting with a slenderness of 60, in order to minimize the buckling effects in the design of compressed elements.

The corresponding sections are shown in Table 3.

Table 3: Cross section geometry for each V_n model

	$t_2[m]$	$t_3[m]$	A $[m^2]$	w $[m^3]$
V_2	0.1	0.1	0.01	0.000167
V_4	0.06	0.06	0.0036	0.000036
V_6	0.04	0.04	0.0016	0.0000107
V_8	0.035	0.035	0.0012	0.0000071

To ensure the safety values according to ULS, the equation 3 was used:

$$\frac{\sigma_{t,ed}}{f_{t,0,d}} + \frac{\sigma_{m,y,ed}}{f_{m,y,d}} + k_m \frac{\sigma_{m,z,ed}}{f_{m,z,d}} \leq 1 \quad (3)$$

In Table 4 are given the main values on the most loaded element, for each V_n model.

In order to simplify the analysis of the Table 5, the Equation 3 is divided in three terms:

- 1st Term: compression or tension effect;
- 2nd Term: bending along the y axis;
- 3rd Term: bending along the z axis.

Table 4: Load values - V_n models

V_n	Tensile force $[kN]$	$M_2[kN.m]$	$M_3[kN.m]$
V_2	1.742	-1.025	-0.547
V_4	4.454	0.057	-0.202
V_6	3.233	-0.050	0.028
V_8	3.273	0.004	-0.030

Table 5: ELU safety design - V_n models

V_n	1st Term	2nd Term	3rd Term	$\sum$Terms
V_2	0.022	0.422	0.210	0.75
V_4	0.158	0.123	0.435	0.72
V_6	0.259	0.365	0.203	0.83
V_8	0.342	0.044	0.322	0.71

We may conclude that for the combination of bending with tension, the bending is more important for the design. However, the bending effect is diminished with the increasing of V_n, which results in higher tension effects.

The chosen cross sections verify the safety values imposed by the ULS design.

It can be seen in Figure 8 that the total weight of the all the timber bars decreases while the frequency, Vn, increases. This happens even with a higher number of structural elements.

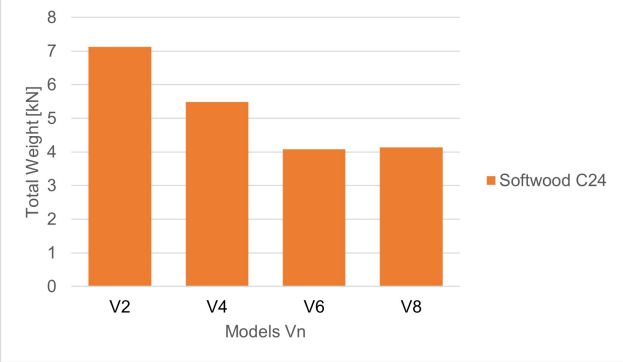

Figure 8: Total weight of the bars for each V_n model

Joints

These elements are made from bamboo which, naturally, have the shape of a cylindrical ring as shown in the Figure 9 with an internal diameter, ϕ_{int}, external diameter, ϕ_{ext}, and a development along the z axis, h. The element's mesh is shown in Figure 10.

Since there are three different types of joints, which intersect 4, 5 and 6 frames, simplified models were developed in order to evaluate the properties for the bamboo. Since this material has not yet been assessed with further detail at a scientific level, and also knowingly of the fact that its resistance varies according to its age wood type, these models were tested for predetermined parameters by [6], as shown in Table 6.

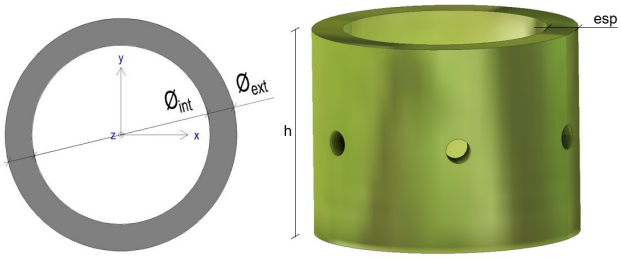

Figure 9: Joint model

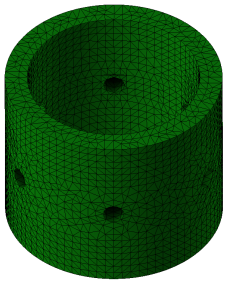

Figure 10: Joint model - mesh

Table 6: Characteristic mechanical properties for bamboo

$f_{y,k}[N/mm^2]$	$f_{t,k}[N/mm^2]$	$E[N/mm^2]$	$\rho[kg/m^3]$
337.5	203	45.475	731

It is verified that for any V_n model, the von Mises comparison tension, σ_{vM}, is lower than the bamboo characteristic tension value. The admissible values correspond to a safety factor between 2 and 4.

Hereinafter, an analysis example is shown for a coupler with 6 holes for a V_4 model, varying the ϕ_{ext} value, for a $h = 60\ mm$ and a $\phi_{int} = 100\ mm$.

Table 7: Analysis results for a 6-hole couplers - V_4

$N_{ed}[kN]$	$\phi_{ext}[mm]$	$esp[mm]$	$\sigma_{vM}[N/mm^2]$	FS
5.60	113	13	172.2	2.0
5.60	122	22	81.7	4.1

4. Case study 2

This second case study corresponds to the underground geodesic domes, as shown in the Figure 11.

Where the combinations of actions for ULS (4) and SLS (5) are:

$$Comb_2 = 1,35 \cdot (dead + soil) + 1.5 \cdot sc \quad (4)$$

$$Comb_{2,ut} = dead + soil + sc \quad (5)$$

Again, the design was performed for both frame and joint elements.

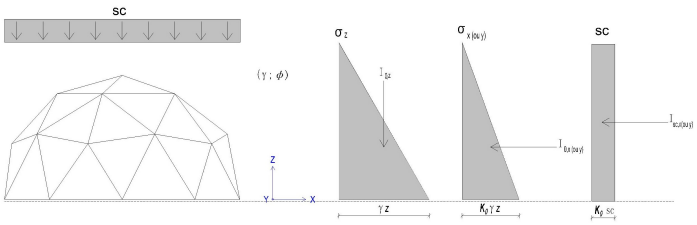

Figure 11: Example of the V_4 model under $comb_2$ (side view)

The loadings on the structures due to the soil pressure were quantified accordingly to the corresponding Eurocode, EC7-1 [7]. The soil parameters used in the model design are shown in Table 8.

Table 8: Soil parameters

$\phi(\circ)$	$\phi_d(\circ)$	$\gamma\ [kN/m^3]$	K_0	γ_ϕ
30	25.7	20	0.5	1.25

Shells

The material chosen for these elements is steel of the class S355, with mechanical properties shown in Table 9.

Table 9: Mechanical properties for the steel class S355

$f_{yk}[N/mm^2]$	$E[kN/m^2]$	$\rho[kg/m^3]$	γ_M
355	2.10 x 10^8	7.85	1.0

The areas in this scenario are structural elements as the one that is shown in the Figure 12, due to the fact that the soil pressures are applied directly onto these. This solution implies the application of a thin metal plate, in order to make the structure watertight.

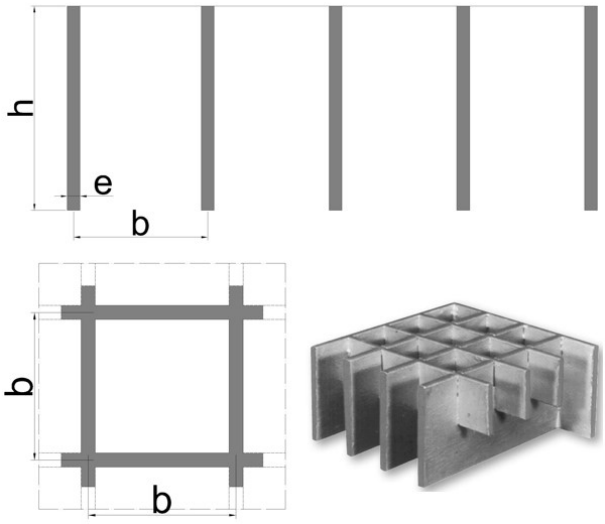

Figure 12: Model of metal grid for the areas, in different perspectives

Conservatively, the design was made for the most solicitated area of each model V_n, according to Figure 13. This design took into account both ULS and SLS limit states.

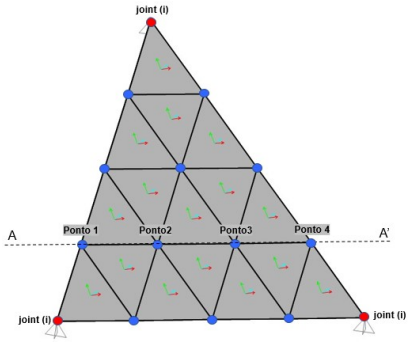

Figure 13: Shell element in analysis

In ULS, the Equation 6 is considered:

$$\sigma_{m,gradil} < f_{y,d} \tag{6}$$

In SLS it is considered that for the alignment A-A' shown in the Figure 13, the value for the maximum admissible displacement corresponds to the condition of the Equation 7.

$$\delta_{max,adm} \leq \frac{L}{300} \tag{7}$$

Where the value of L is contained within the points number 1 and 4.

The parameters for the type of metal grid considered in each structure V_n, are defined in Table 10.

Table 10: Geometrical properties considered in the models V_n

	V_4	V_6	V_8
e (mm)	2	2	2
h (mm)	80	50	40
b (mm)	50	50	50

In the Table 11 it is confirmed that the parameters in the Table 10 fulfil the safety verifications for both limit states.

Table 11: Tensions and displacements in the area V_n

	V_4	V_6	V_8
$\sigma_{m,gradil}[N/mm^2]$	319	287	234
$\delta_{max,adm}[mm]$	3	2	1
$\delta_{max,obtido}[mm]$	[0.4;0.6]	[0.2;0]	[0.1;0.1]

Frames

The frame elements are considered to be in steel of the class S275 with a square tubular cross section, and the design was made according to the general Eurocode EC1 [4] rules, and also the one associated to the type of material, in this case, EC3 [8].

The critical evaluation for these elements is the interaction of combined bending with axial compression, therefore, it is necessary to verify the condition shown in the Equation 8.

$$\frac{N_{ed}}{\chi N_{Rk}} + k_{yy}\frac{M_{2,ed}}{\chi_{LT} M_{y,Rk}} + k_{yz}\frac{M_{3,ed}}{M_{z,Rk}} \leq 1 \qquad (8)$$

Where χ_{LT}=1, because for tubular sections there is no lateral torsion. The remaining interaction parameters are obtained from the EC3. In Table 12 are given the defined values for the frame element geometry, based on the previously mentioned slenderness factor of 60.

Table 12: Definition on the frame cross section - V_n models

	t_3,t_2 $[m]$	t_f,t_w $[m]$
V_4	0.08	0.008
V_6	0.06	0.004
V_8	0.04	0.004

The force values for the most unfavourable element of each V_n model are given in table 13.

Table 13: Force values - V_n models

V_n	Tensile Force $[kN]$	$M_2[kN.m]$	$M_3[kN.m]$
V_4	-50.83	6.957	-5.987
V_6	-29.67	2.019	1.938
V_8	-19.942	0.848	0.836

To simplify the analysis of the Table 14, once more, the Equation 8 is divided in three terms:

- 1st Term: compression effect;
- 2nd Term: bending along the y axis;
- 3rd Term: bending along the z axis.

Table 14: ELU safety design - V_n models

V_n	1st Term	2nd Term	3rd Term	$\sum$Terms
V_4	0.108	0.444	0.229	0.78
V_6	0.144	0.382	0.221	0.75
V_8	0.139	0.372	0.220	0.73

We may conclude that for these sections (Table 14), when compared to the compression, the combined bending is more important for the frame design, while subjected to the high soil pressures.

For the case study 2, it is shown in Figure 14 the total steel weight of the structure, making a comparison between the adopted solution - with frames in SHS steel profiles and the shells in metal grid - and an alternative option, if the choice for the shells would have been steel plates - instead of the metal grid. It can be seen that the structural weight of this alternative would be much higher than the adopted solution with the metal grating, especially taking into account that to withstand the soil pressures, it would require steel plates of thickness within the range of 1.5 cm up to 3 cm.

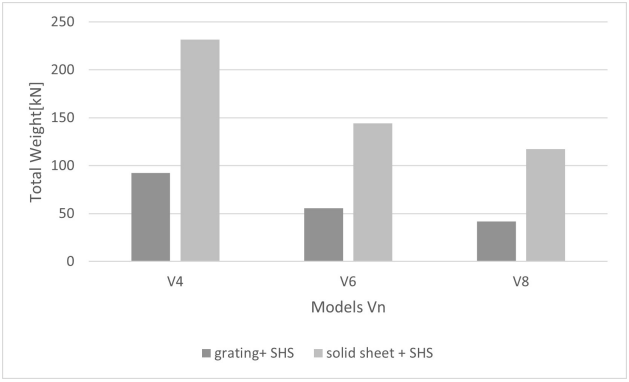

Figure 14: Total weight of the bars for each model V_n

5. Conclusion

The general conclusion for both case studies is that, when compared with tension/compression, the bending forces are more conditioning in any model with a shorter or higher frequency, for both area and frame elements. At the joints this doesn't apply, since these are only subjected to axial loading.

For the surface level dome's scenarios, the V_4 model is the more feasible, since it has a more balanced relationship between the number of bars and its corresponding length, while maintaining a cross section of reasonable dimension.

For the underground dome's scenarios, it's inconclusive which is in fact the best model, nevertheless, it can be stated that the V_4 model may require shells with high areas, which implies a heavier metal grating, when compared to the V_6 and V_8 models, which have smaller areas.

In terms of material selection, it may be concluded that it's possible to consider timber as a structural material for these types of geodesic structures, as long as the applied forces and the environmental conditions are kept within a reasonable level. Steel remains a valid option, since it's a strong and resistant material, more easily applied in other situations with a higher level of forces. It was also introduced the bamboo material and, although its performance was not evaluated in detail, it's possible to assume that it will be a material with an important potential in the future of construction, due to its resistance.

This document only refers, in a concise manner, the in-depth analysis that was made for both of these case studies, which may be viewed with further detail in [9].

References

[1] E. J. Fuller, D E Buckminster; Applewhite. *Synergetics: Explorations in the Geometry of Thinking*. 1976.

[2] Edward Zechmann. Make Icosahedron, 2008.

[3] CEN. Eurocodigo 1 : Acções em estruturas — Acções gerais — Part 1-4 : Acções do vento. 2010.

[4] CEN. Eurocódigo 1 - Acções em estruturas. 2009.

[5] CEN. Eurocódigo 5 – Projecto de estruturas de madeira Parte 1-1: Regras gerais e regras para edifícios. 2011.

[6] Anil Shastry and Sujatha Unnikrishnan. Investigation on Elastic Properties of Bamboo and Behavior of Bamboo Reinforced Concrete Beams. *International Journal of Earth Sciences and Engineering*, 10(02):304–312, 2017.

[7] CEN. Eurocódigo 7 - Projecto de estruturas geotécnicas Parte 1: Regras gerais. 1, 2004.

[8] CEN. Eurocódigo 3 – Projecto de estruturas de aço Parte 1-1: Regras gerais e regras para edifícios. 1993.

[9] Raquel Vestia Ribeiro. Modelação e Análise de Cúpulas Geodésicas, 2020.